Investigation of Static Microisolators in Wind Tunnel Tests and Validation of CFD Cage Model

Gerald L. Riskowski, Ph.D., P.E.
Member ASHRAE

Farhad Memarzadeh, Ph.D., P.E.

ABSTRACT

The results from an experimental and numerical study of a known mouse cage (static microisolator type) placed in a wind tunnel are presented. The study involved the collection of experimental airflow data and the use of these data in the validation of the computational fluid dynamics (CFD) cage model. This validation was important as it then allowed the CFD cage model to be used to represent cages in whole room simulations, the basis of a study presented in Memarzadeh (1998). The validation exercise indicated that the CFD cage model exhibited the same air flow characteristics as the experimental cage, accounting for the spread of the experimental data. The consequence of this is that when the cage model is placed in a CFD model of a whole animal room facility, a good degree of confidence can be placed in the values obtained for the considered variables, namely, CO_2, NH_3, cage temperature, and RH.

INTRODUCTION

A series of experimental scenarios were defined to consider a known mouse cage (static microisolator type) placed in a wind tunnel. This study was conducted by the National Institutes of Health (NIH) in collaboration with a major Midwest university. The primary objective of the experimental measurements was to create and measure various airflows within the mouse cage in such a manner as to lay the groundwork for determining the boundary conditions for a computational fluid dynamics (CFD) analysis of the cage. In particular, a series of CFD models were constructed to simulate the cage wind tunnel experiments. The primary reason for the validation of the CFD model of the cage against experimental data was to obtain an appropriate set of boundary conditions to represent the cage in whole room simulations, the basis of a study presented in Memarzadeh (1998). The CFD code used was produced by a company that specializes in software for the calculation of airflow, heat transfer, and contamination distribution in building environments.

This consideration of the CFD cage model was a key aspect of the study. Without the extensive validation of the cage model, the numerical results obtained for such cage parameters as CO_2, NH_3, air temperature, and relative humidities (RH) would be subject to considerable doubt. In particular, if the CFD cage model was seen not to match experimental airflow data, then the cage parameters, which are subject to airflow distributions, would be predicted incorrectly.

EXPERIMENTAL APPARATUS

The apparatus used in this series of experimental scenarios was kept relatively constant throughout, with the main difference being the representation of the mice within the cage.

The wind tunnel cross section was 0.40 m wide by 0.50 m deep (15.75 in. × 20 in.). It was 1.72 m (68 in.) long with a 0.80 m (32 in.) long test section in the center. Room air entered the wind tunnel through a furnace filter (0.41 m × 0.50 m × 0.025 m; 16 in. × 20 in. × 1 in.), then passed through three perforated metal screens (60%, 40%, then 33% open area) that acted as a settling means so airflow approaching the test section was uniform. The inlet filter was placed 0.10 m (4 in.) from the end of the wind tunnel and the outlet filter was 0.43 m (17 in.) from the other end. The first metal screen was 0.10 m (4 in.) from the inlet filter, and the screens were spaced 0.10 m (4 in.) apart. A schematic of the wind tunnel is shown in Figure 1.

Gerald Riskowski is a professor at the University of Illinois, Urbana, Ill. **Farhad Memarzadeh** is chief of the Technical Resource Group, National Institutes of Health, Bethesda, Md.

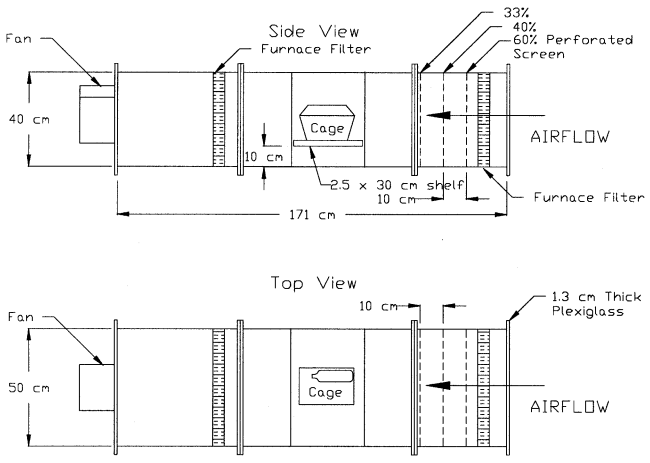

Figure 1 *Parallel cage orientation layout.*

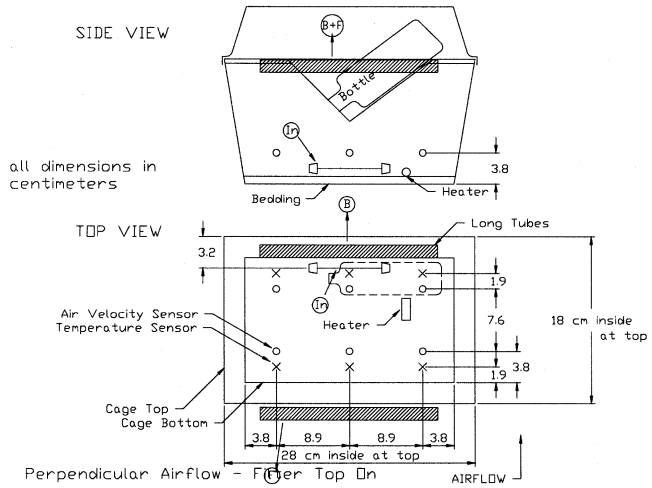

Figure 2 *Sensor, air inlet, and sampling location for cage perpendicular to horizontal airflow. Mouse heater representation: DMH.*

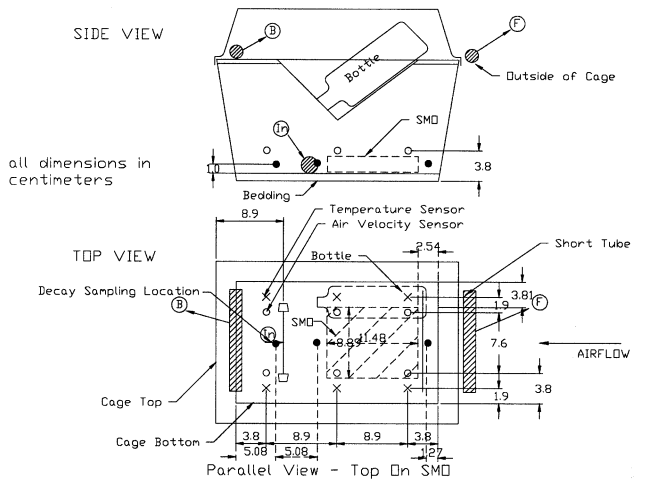

Figure 3 *Sensor, air inlet, and sampling location for cage parallel to horizontal airflow. Mouse heater representation: SMO.*

The instrumented mouse cage was a standard shoebox mouse cage with approximate top dimensions of 0.18 m wide by 0.28 m long by 0.13 m high (7 in. × 11 in. × 5 in.) (see Figures 2 and 3). The filter top was the high profile type and the filter was 2.1 oz/yd^2, 12 mils thick. The cage had approximately 0.0125 m (0.5 in.) of hardwood shaving bedding on the floor and contained a wire rack, water bottle, and simulated feed.

The cage also contained one of two mouse heater representations: a simple, small electric heater, that will be known hereafter as the default mouse heater (DMH), and a more realistic representation of the physical presence and heat transfer characteristics of a mouse huddle, that will be know hereafter as the simulated mouse object (SMO) (shown in Figure 4). In the cases that included the DMH, the cage had an electric heater placed on the bedding toward the front of the cage, which produced heat equivalent to the total heat production of five mice weighing 0.02 kg (0.44 lb) each, or 2.3 W in total. Heat production simulated was based on the ASHRAE (1997) equations:

$$ATHG = 2.5\ M$$

$$M = 3.5\ W^{0.75}$$

where

ATHG = average total heat production from laboratory animal, W/animal;

M = metabolic rate of animal, W/animal;

W = mass of animals, kg.

The DMH was a 200 ohm precision resistor with approximately 21.5 V of direct current from a regulated, filtered DC power supply.

In the cases that included the SMO, the cages included a more accurate mouse huddle representation, which was placed within the cage at a location centered width-wise and toward the front one-third in the same location as the resistor heater (see Figure 3). The SMO was designed to simulate five mice

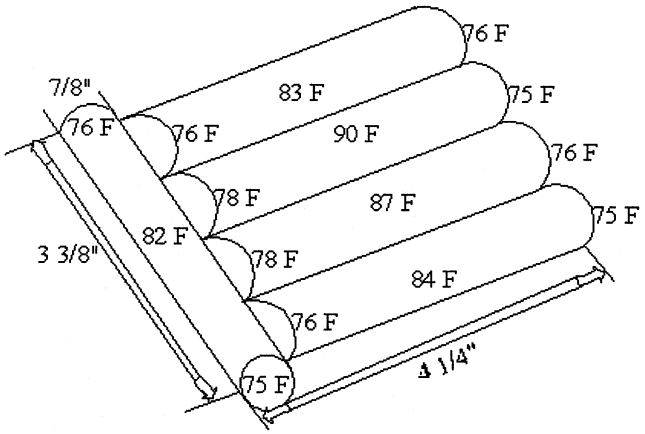

Figure 4 *Simulated mouse object (SMO) with surface temperatures and dimensions.*

for volume obstruction, sensible heat production, and surface temperature. The mice were simulated using 0.022 m (7/8 in.) outside diameter PVC pipe. The pipe had a wall thickness of 0.0024 m (3/32 in.) and was cut to 0.043 m (1-11/16 in.) lengths. The ends of the pipe were covered with duct tape and plastic caps. Sensible heat was simulated using one 200 ohm precision resistor powered at 9 volts per pipe. Before starting the experiment, the surface temperature of the SMO was measured several times at various locations, using an infrared thermometer (see Figure 4), and shown to closely correspond to that found on the fur of the dorsal surface of mice by Gordon et al. (1997), about 26.7°C (80.0 °F). Justification for the physical sizing of the SMO is given in Memarzadeh (1998).

In both mouse heater representations, a voltage regulator was used to produce the voltage. The voltage was constantly monitored using a multimeter. Resistance was checked at the beginning of each experiment with the multimeter to guarantee the resistor was in working order.

The cage was instrumented to measure air velocities approaching or moving past the cage on all four sides, at approximately the top edge of the cage or the lip of the top. An air velocity sensor was placed on each of the four sides at approximately 0.02 m (0.75 in.) distance out from the cage at the mid-length of each side. Air velocities, temperatures, and air exchange rates were measured inside the cage. Air velocities and temperatures were measured with thermistor-based air velocity sensors and type-T thermocouples, respectively. Six air velocity sensors were placed approximately 0.025 m (1 in.) above the bedding and uniformly spaced around the cage at this level. Six thermocouples were placed approximately 0.025 m (1 in.) from each air velocity sensor at the same height. A data logger collected cage sensor outputs.

Rates of air changes per hour (ACH) in the cages were calculated from gas (CO_2 or SF_6) concentrations sampled from tubes placed at appropriate locations within the cages. When tunnel air approaches the cage, air is drawn from one part of the cage and fresh air enters the cage at another location. Therefore, to assess the air change rate, air has to be sampled at both the entering and exiting locations of the cage. Smoke sticks (titanium tetrachloride) were placed into the cage to visually determine the locations where air entered and exited the cages in order to locate the sampling tubes.

The tracer gas, either CO_2 or SF_6, was introduced into the cage through diffuser stones located near the bedding of the cage. In the case of SF_6 experiments, the tubing used was polytetrafluorethylene to prevent gas absorption/readmission.

Exact sensor locations, cage dimensions, sampling tubes, and cage locations within the wind tunnel are indicated in Figures 2 and 3.

EXPERIMENTAL DATA SETS CONSIDERED

There were nine series of experimental scenarios considered in this project, as listed in Table 1.

TABLE 1
Table of Cage Condition Experimental Series

Series Set	Tracer Gas	Injection Rate (L/ min)	Sampling Method	Mouse Heater Type	Cage Orientation	Tunnel Air Velocity Range (fpm)
Base	CO_2	1.0	Steady	DMH (On/ Off)	Par, Perp, Vert	15 – 100
One	CO_2	0.1	Steady	DMH (On only)	Par, Perp	15 – 50
Two	SF_6	0.1	Steady	DMH (On only)	Par, Perp	15 – 50
Three	CO_2	0.1	Steady	DMH (On/ Off)	Par, Perp, Vert	20, 40
Four	CO_2	0.1	Steady	SMO (On only)	Par, Perp, Vert	20, 30, 40
Five	CO_2	0.1	Decay	SMO (On only)	Par, Perp, Vert	20, 30, 40
Six	CO_2	0.1	Steady	DMH (On/ Off); SMO (On Only)	Par, Perp	20,40
Seven	CO_2	0.1	Steady	DMH (On/ Off); SMO (On Only)	Par, Perp	20, 40
Eight	CO_2	0.1	Steady	SMO (On Only)	Par, Perp	30

Series Set Base

In this series of experiments, the tracer gas used to determine the ventilation rate was exclusively 99.8% pure CO_2 that was injected (and sampled) at a rate of 1 L/min into the cage. The approaching wind tunnel air impacted the cage in three different orientations: the parallel orientation, in that the tunnel air moved horizontally toward the front edge of the cage; the perpendicular orientation, in that the tunnel air moved horizontally toward the side of the cage; and the vertical orientation, in that the tunnel air moved vertically downward toward the top of the cage. In each orientation, the air velocities approaching the cage were 0.075, 0.10, 0.15, 0.20, 0.25, 0.3, 0.35, 0.40, 0.45, and 0.5 m/s (15, 20, 30, 40, 50, 60, 70, 80, 90, and 100 fpm, respectively).

Series Sets One and Two

It was decided that the injection rate of CO_2 utilized in the series set base may have been too large in comparison with the likely gaseous generation rates from the mice in the actual physical case and that the magnitude of the injection could affect the flow field conditions within the cage, i.e., the gas would no longer act as a tracer gas. Also, it was decided that the higher end of the velocity range chosen, i.e., 0.3 m/s (60 fpm) and above, was unlikely to be present in the animal room facility close to the cages.

In series sets one and two, therefore, the injection rate was reduced to more realistic levels, and the tunnel approach velocity range was clipped at 0.25 m/s (50 fpm). In both series set one and two, the injection (and sampling) rate was set at 100 mL/min; in series set one, the tracer gas used was 99.8% pure CO_2, and in series set two, the tracer gas used was 4.99 ppm SF_6. The tests ran at 0.075, 0.10, 0.15, 0.20, and 0.25 m/s (15, 20, 30, 40, and 50 fpm, respectively). The parallel and perpendicular orientations were both considered.

Series Set Three

In the third series set, the parallel cage orientation with CO_2 tracer gas was repeated with the heater on and the heater off for only the 0.10 and 0.20 m/s (20 and 40 fpm) air velocities to determine if the heater had a significant effect.

Series Sets Four and Five

Series sets four and five compared two tracer gas methods: the constant injection method and the decay method. In both methods, CO_2 was injected at 100 mL/min (0.00353 ft^3/min) in the same locations as in series set one. A simulated mice obstruction (SMO) occupied approximately the same volume, produced the same sensible heat, and had approximately the same surface temperature as five mice in a tight group. The tests were run at three approach air velocities, 0.10, 0.15, and 0.20 m/s (20, 30, and 40 fpm, respectively), and three cage orientations to airflow (parallel, perpendicular, and vertical).

It should be noted that the primary reason for the series set five experimental tests was to replicate and expand the work performed by Keller et al. (1989). In particular, the authors measured decay data for a cage that was orientated in the parallel direction and was subject to an approach velocity of 0.08 m/s (16 fpm). The cage used in the Keller et al. (1989) study was very similar to that used in this one. The emphasis of this experimental data set is to demonstrate that the experimental procedure being utilized in the current study was technically correct and that the cage considered was representative of a typical mouse cage.

Series Sets Six and Seven

Series sets six and seven were conducted with the filter lid on but with a seal around the lip edges so all airflow through the cage passed through the filter or with the filter lid sealed and the lip edge open. These results were compared to the results from series set three. The tests were similar to series set three except for the sealed edge and top; only the constant injection method was used, and only the 0.10 and 0.20 m/s (20 and 40 fpm) air velocities were used with only parallel and perpendicular airflow orientations. Also, during part of this series set, the SMO was introduced into the cage in place of the resistor, as a heat source. Data were collected using a randomized complete block design with the lid condition being blocked. The SMO was always allowed to produce heat. The heater state and air velocity levels were randomized within each lid condition block.

Series Set Eight

Series set eight was conducted with pairs of cages together. In these tests, two cages were considered side by side for both the parallel and perpendicular cage orientations with the spacing between the cages set to that which the cages would experience in an animal facility room. In particular, the spacing between the cages in both cases was set to 0.0281 m (1.11 in.). Only one tunnel velocity, 0.15 m/s (30 fpm), was considered for each orientation. Instrumentation was included in one cage only. The other cage was left basically empty.

EXPERIMENTAL PROCEDURES

The description of the procedures for the various experimental data sets is too detailed to be included here. The reader is directed to Section 4 of Memarzadeh (1998) for a full description of the procedures for the different experimental series.

METHODOLOGY FOR CALCULATION OF CAGE ACH

The cage ventilation rate for all steady-state injection cases was calculated from Bennett and Myers (1982):

$$Q = (C_S Q_S \quad C_O Q_S)/(C_O \quad C_I)$$

where

Q = cage ventilation rate, ft^3/min;

C_S = CO_2 or SF_6 concentration of tracer gas: 99.8% for CO_2, 4.998 ppm for SF_6;

Q_S = rate of tracer gas injection and air sampling from cage: 0.0353 ft^3/min for 1 L/min cases; 0.00353 ft^3/min for 100 mL/min cases;

C_O = CO_2 or SF_6 concentration of air exiting cage, %;

C_I = CO_2 or SF_6 concentration of air entering cage, %.

The cage ventilation rates were adjusted to standard air density conditions at sea level (barometric pressure = 29.92 in. Hg) and 70°F by multiplying by a factor K:

$$K = (29.92/\text{barometric pressure, in. Hg}) \times ((490 + \text{air temp.°F}) / (460 + 70)).$$

This procedure was followed for both the experimental and CFD results.

CONSIDERATION OF DECAY (SERIES SET FIVE) RESULTS

The decay data are important in that they can be compared with previous work. In the case of a decaying concentration within a volume, the level of concentration remaining can be calculated from

$$C = Co\ e^{\ t}$$

where

C = % concentration, at time t;

Co = % initial concentration, at $t = 0$;

= decay constant.

As the level of initial concentration varies from case to case, it is more convenient to normalize the decay such that the initial concentration is considered as 100%. The time taken to decay by a certain amount can then be tabulated. Table 2 compares the time taken to decay the concentration by 90%, 95%, and 99% for the cage considered in Keller et al. (1989) and the parallel orientation cases considered in series set five.

Further, Figure 5 displays the comparison between the series set five parallel orientation results and the results presented in Keller et al. (1989) with the concentration levels normalized such that the initial concentration is considered as 100%.

TABLE 2
Time Taken to Decay Concentration by 90%, 95%, and 99% for the Keller et al. (1989) Cage, and Series Set Five: Parallel Orientation Results

Tunnel Velocity (FPM)	Time To Decay (min)		
	90%	95%	99%
Keller, White, Snyder, and Lang (1989) (at 16 fpm)	18.27	23.77	36.54
20	16.69	21.27	33.27
30	12.38	16.11	24.76
40	11.29	14.68	22.57

The plot in Figure 5 and Table 2 clearly show that the current data are entirely consistent with those data presented in the previous study. There are two conclusions to be drawn from this comparison:

- The experimental procedure followed in this section of the study, as well as the method for determining the decay characteristics of the cage, were consistent with other experimental studies.
- The cage used in this section of the study is a typical microisolator type cage, not a cage fabricated to exhibit certain characteristics.

CFD SIMULATIONS AND VALIDATION AGAINST EXPERIMENTAL DATA

A series of CFD models were constructed to simulate the cage wind tunnel experiments. The accurate modeling of the cage was an important stage in the project. In particular, the CFD cage model, as validated against the experimental data obtained in the wind tunnel, was used in later CFD animal research facility models as part of the rack representation.

The two sets of boundary conditions that are of most concern are those associated with the transfer mechanisms into and out of the cage, namely, the side cracks and the top of the cage, which includes the filter.

Description of CFD Models

All the models contained the same basic components and modeling philosophy; changes between the models reflected the different experimental procedures. The models were all constructed using a CFD code and simulated by super computers.

The walls of the tunnel were specified to define the shape of the experimental wind tunnel. A typical CFD model

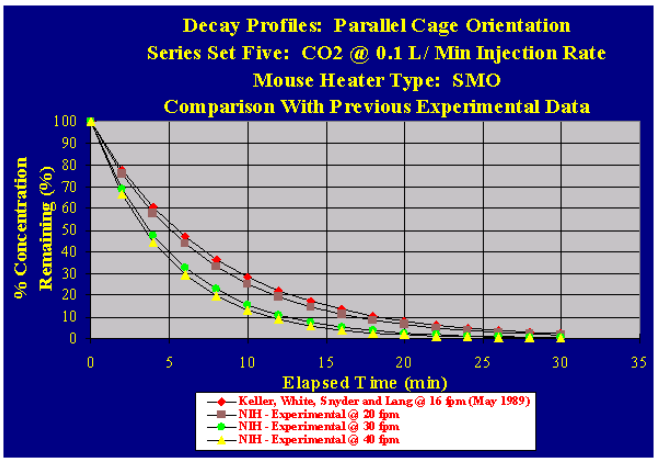

Figure 5 *Comparison of series set five: Parallel orientation sampling method results and results from Keller et al. (1989).*

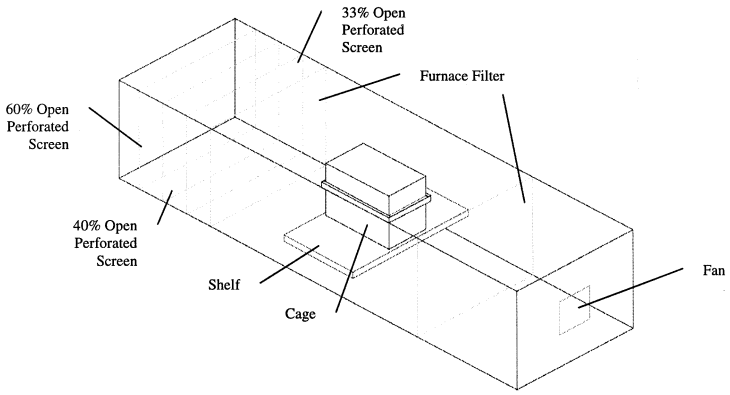

Figure 6 *Parallel cage orientation CFD model.*

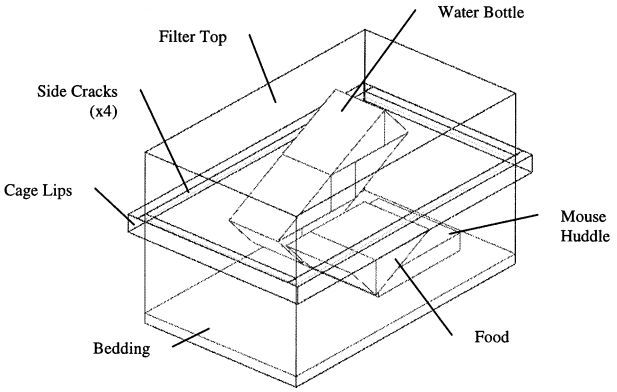

Figure 7 *CFM model of single cage. Sampling tubes and injection diffuser stones not shown. Mouse heater representation: SMO.*

for the tunnel is shown in Figure 6. The three screens and two filters in the tunnel were modeled using 0.4 m by 0.5 m (15.75 in. × 20 in.) planar resistances. The loss coefficients for each were set according to the free area ratio of the object. The values are listed in Table 3 and are based on Idelchik (1989).

The shelf on which the cage sat was defined as a rectangular block of dimensions 0.025 m by 0.30 m by 0.50 m (1 in. × 11.8 in. × 20 in.). The shelf was located 0.10 m (4 in.) from the floor of the tunnel for the parallel and perpendicular orientation experimental measurements, with the center of the shelf located at the center of the tunnel section. In the vertical orientation experiments, the shelf was located centrally within the tunnel.

Placed on the shelf was the CFD model representation of the cage. A typical representation of the cage, without instrumentation, is shown in Figure 7. The dimensions of the cage were set as 0.27 m by 0.16 m by 0.21 m (10.7 in. × 6.38 in. × 8.39 in.); these dimensions retained the same volume as in the physical case. The sides of the cage were modeled as thin plates, with the thickness and conductivity of the plates set to those of the cage polycarbonate. The bottle was represented using a combination of rectangular prisms and cuboid blocks. The volume of the bottle was retained, as was the location of the bottle in the cage. A food supply was modeled using two triangular prisms. The bedding was represented as a rectangular block with dimensions of 0.27 m by 0.16 m by 0.013 m (10.7 in. × 6.38 in. × 0.5 in.). The alternative representations of the mice heater were modeled using rectangular blocks. In particular, the original heater was modeled as a 0.0159 m by 0.0032 m by 0.0032 m (5/8 in. × 1/8 in. × 1/8 in.) block, with the heat flux set to 2.3 W, while the huddled mice were modeled as a block of dimensions 0.11 m by 0.086 m by 0.022 m (4 1/4 in. × 3 3/8 in. × 7/8 in.), with the surface temperature set to 26.7°C (80.0°F).

TABLE 3
Free Area Ratios and Loss Coefficients Used for Tunnel Straightening Media

Device	Free Area Ratio	Loss Coefficient
Screen1	0.6	2.00
Screen2	0.4	8.25
Screen 3	0.33	14.35
Filters 1, 2	0.5	4.00

There are two transfer mechanisms for the air and tracer gas to enter/ leave the cage, namely, the top of the cage, which includes filter media, and the side cracks of the cage.

The top of the cage has two constituent parts that had to be represented using CFD boundary conditions: the filter media and the top of the cage itself, which consists of regular arrays of holes in the polycarbonate material. The filter material was identified as 12 mils, 2.1 oz/ yd^2. Using manufacturer's data, a pressure drop vs. wind tunnel speed graph could be plotted in Figure 8. The profile was then approximated to a polynomial expression that could be converted to CFD boundary conditions. In particular, the polynomial expression can be expressed as

$$DP = 70.277\, v^2 + 307.37\, v$$

As the average velocities through the filter are relatively small (on the order of 0.0008 m/s [0.17 cfm]), the linear contribution dominated the pressure drop. The loss coefficients were set appropriately for each boundary condition to replicate the polynomial expression. As the flow through the filter media is laminar, the turbulent viscosity at the plane of the media was reduced to very low levels. To achieve this, the value of k (the turbulent kinetic energy) was set at 0.00001 at the planar source, while (the rate of dissipation of k), was set to 100,000.

The cage top material itself was represented through the calculation of the free area ratio of the top surface and the addition of the loss coefficient to the planar resistance term. The free area ratio was calculated to be 0.35, which gives a loss coefficient of 12.35 (Idelchik 1989).

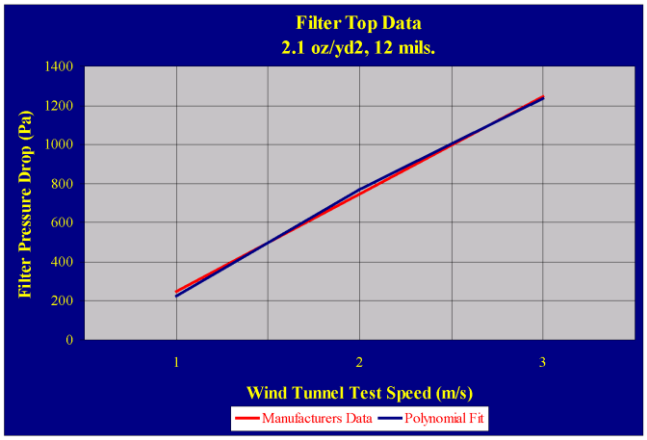

Figure 8 *Filter material test data and polynomial approximation.*

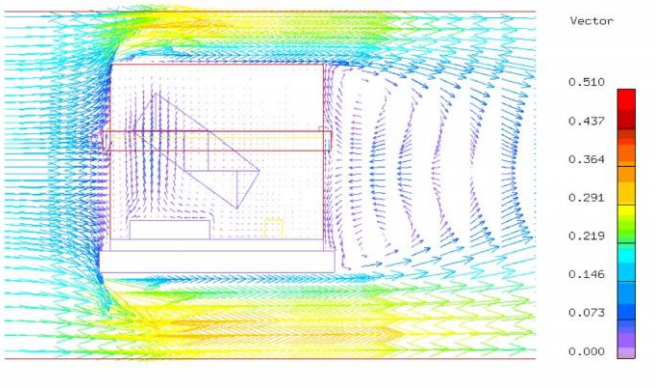

Figure 9 *Close-up plot of the vector field at mid-plane of tunnel. Series set six: parallel orientation, heater on (SMO), 40 fpm (0.2 m/s).*

The settings for the side crack boundary conditions were the most problematical to specify because of physical uncertainties. In particular, the top lid of the cage does not fit well on the lower section of the case because the meshing is often deformed. The first step was to define these cracks as planar resistances of height 0.0064 m (¼ in.). Initially using the results of the series set base experiments, the values for the loss coefficients on the side cracks were varied until the predicted CFD values for the cage ACH reasonably matched the experimental data over a range of tunnel velocities for each of the three orientations. These loss coefficient values were then tested against the lower injection rate experimental series (series sets one to four, to eight) to ensure good agreement. Any adjustments to the loss coefficients were then tested over a range of experimental data sets to ensure that the values were applicable to all possible conditions in which the cage could be presented within the animal facility room environment.

Results from CFD Simulations

In this section, variable plots from a typical cage will be considered, and then a comparison of the CFD results with the experimental data will be presented.

Plots from Typical Cage CFD Simulation. A single CFD simulation will be considered to indicate the physical features that can be predicted using CFD, which are otherwise difficult to determine using experimental procedures. In particular, CFD allows the determination of flow patterns within the cage, as well as temperature and concentration distributions.

The close-up plot of the vector field at the plane halfway through the tunnel for series set six, parallel orientation, heater on (SMO), 40 fpm (0.2 m/s) case is shown in Figure 9. Note that the key accompanying the plot indicates speed in m/s (to convert to fpm, multiply by 200). Externally from the cage, the most prominent feature is the recirculation region immediately behind the cage. Internally, the main feature is the buoyant plume resulting from the SMO. However, it is noticeable that apart from the plume, there are few flow patterns present within the cage of any great magnitude. In particular, although there is obviously strong external flow that is impinging directly onto the side of the cage, relatively small amounts of flow actually enter it.

The equivalent close-up plots of the temperature and CO_2 concentration fields are shown in Figures 10 and 11, respectively. Note that the keys indicate the temperature in °C and concentration in kg of species/kg of air (to convert to ppm, multiply by 1,000,000*(28.96/44)), respectively. The temperature plot shows the distinct plume resulting from the SMO. This plume dominates the distribution of the concentration also, as the CO_2 is entrained into this flow feature. The concentration plot also indicates the clear stratification of the CO_2 in the cage. That is due to the density difference between the CO_2 and air. This stratification makes the matching of the CFD results to the experimental data difficult, as relatively small spatial changes result in marked differences in the level of concentration.

Comparison of CFD Results vs. Experimental Data. Presented in Tables 4 to 14 are a series of comparisons between the experimental data sets and equivalent CFD simulation cage ACH for the chosen optimal values for the cage side crack loss coefficients. Note that, because of time constraints, only a representative sample could be considered from the wide range of experimental data available. The focus of the sample was to pick orientations that the cage was more likely to experience in the animal facility room environment, in particular, parallel cage orientation and appropriate air velocities, in particular, 40 fpm (0.2 m/s) and below.

A complete listing of the experimental cage ACH data is given in Memarzadeh (1998).

The comparisons show good agreement between the experimental data and CFD simulation results for the range of experimental series considered. In the majority of cases considered, the difference between the experimental and CFD results is under 20%. This error can be considered reasonable for this set of validation and calibration exercises. In particu-

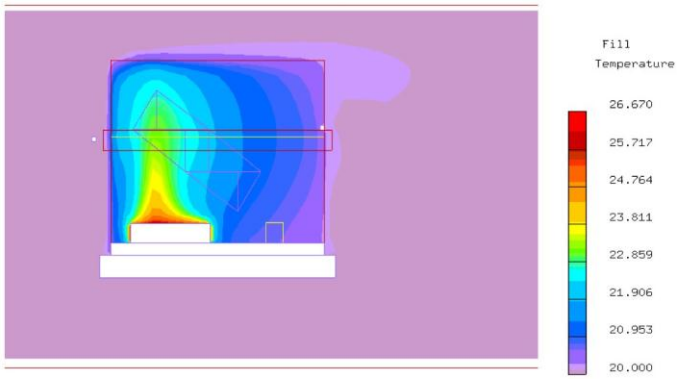

Figure 10 *Close-up plot of the temperature field at mid-plane of tunnel. Series set six: parallel orientation, heater on (SMO), 40 fpm (0.2 m/s).*

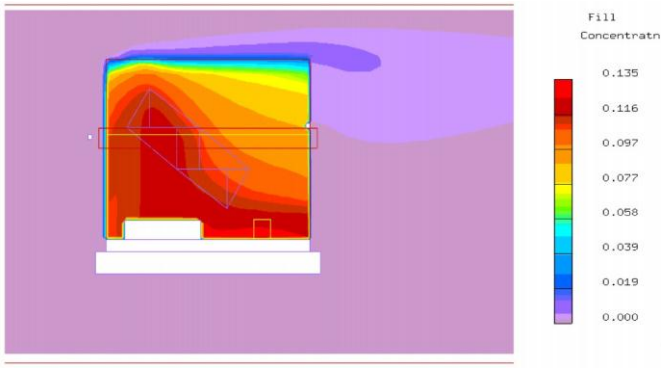

Figure 11 *Close-up plot of the CO_2 concentration field mid-plane of tunnel. Series set six: parallel orientation, heater on (SMO), 40 fpm (0.2 m/s).*

lar, the CFD results show that the calculated value for the cage ACH is sensitive to the exact location of the sampling tubes and the sampling tube holes themselves—this is because of the stratification of the CO_2 or SF_6 concentrations in the cages (see Figure 11). Relatively small variations from the quoted location of the experimental sampling tubes would translate to errors in the CFD calculation. Further, as Table 4 demonstrates, some level of error should be accepted in the experimental procedure.

CONCLUSIONS

A series of experimental scenarios were defined to consider a known mouse cage (static microisolator type) placed in a wind tunnel. The primary objective of the experimental measurements was to create and measure various airflows within the mouse cage in such a manner as to lay the groundwork for determining the boundary conditions for computational fluid dynamics (CFD) analysis of the cage. In particular, a series of CFD models were constructed to simulate the cage wind tunnel experiments.

The primary conclusions of the study are:

- On consideration of the decay tracer gas results, the cage considered in this study and the experimental procedure followed are consistent with previously published studies, in particular Keller et al. (1989).
- The CFD cage model exhibits the same air flow characteristics as the experimental cage, accounting for the spread of the experimental data. This means that when the cage model is placed in a CFD model of a whole animal room facility, a good degree of confidence can be placed in the values obtained for the considered variables, namely, CO_2, NH_3, cage temperature, and RH.

REFERENCES

ASHRAE. 1997. *1997 ASHRAE Handbook—Fundamentals*. Atlanta: American Society of Heating, Refrigerating and Air-Conditioning Engineers Inc.

Bennett, C.O., and J.E. Myers. 1982. *Momentum, heat and mass transfer*, 3d ed. Chemical Engineering Series. New York: McGraw-Hill, Inc.

Gordon, C.J., P. Becker, and J.S. Ali. 1997. *Behavioral thermoregulatory responses of single- and group-housed ice*. Neurotoxicology Division, National Health and Environmental Effects Research Laboratory, U.S. Environmental Protection Agency, Physiology and Behavior (accepted for publication).

Idelchik, I.E. 1989. *Flow resistance: A design guide for engineers*, E. Fried, ed. New York: Hemisphere Publishing Corp.

Keller, L.S.F., W.J. White, M.T. Snyder, et al. 1989. An evaluation of intra-cage ventilation in three animal caging systems. *Lab. Anim. Sci.* 39: 237-242.

Memarzadeh, F. 1998. *Ventilation design handbook on animal research facilities using static microisolators*. Bethesda, Md.: National Institutes of Health, Office of the Director.

TABLE 4
Comparison of CFD Results Against Series Set Base: Parallel Orientation Results

Tunnel Velocity (FPM)	Ventilation Rate (CFM) 1 l/min CO_2 Parallel – Heater On		
	CFD	Series Set Base	Series Set Base (Repeat)
20	0.15	0.19	--
30	0.17	0.21	0.18*

* The % difference between the two separate experimental readings is 14.3%.

TABLE 5
Comparison of CFD Results Against Series Sets Two: Parallel Orientation, SF_6 Results

Tunnel Velocity (FPM)	Ventilation Rate (CFM) 0.1 l/min SF_6 Parallel – Heater On	
	CFD	Set Two
20	0.04	0.04
30	0.05	0.05
40	0.06	0.06

TABLE 6
Comparison of CFD Results Against Series Sets Two: Perpendicular Orientation, Heater On, SF_6 Results

Tunnel Velocity (FPM)	Ventilation Rate (CFM) 0.1 l/min SF_6 Perpendicular – Heater On	
	CFD	Set Two
20	0.05	0.04
30	0.05	0.05
40	0.06	0.05

TABLE 7
Comparison of CFD Results Against Series Sets One and Three: Parallel Orientation, Heater On Results

Tunnel Velocity (FPM)	Ventilation Rate (CFM) 0.1 l/min CO_2 Parallel – Heater On		
	CFD	Series Set One	Series Set Three
20	0.07	0.07	0.08
30	0.09	0.10	0.11
40	0.10	0.10	0.13

TABLE 8
Comparison of CFD Results Against Series Sets Three: Parallel Orientation, Heater Off Results

Tunnel Velocity (FPM)	Ventilation Rate (CFM) 0.1 l/min CO_2 Parallel – Heater Off		
	CFD	Series Set Three	Series Set Three (Repeat)
20	0.10	0.09	--
30	0.10	0.12	0.09*
40	0.12	0.15	--

* The % difference between the two separate experimental measurements is 25%.

TABLE 9
Comparison of CFD Results Against Series Sets Three: Perpendicular Orientation, Heater On Results

Tunnel Velocity (FPM)	Ventilation Rate (CFM) 0.1 l/min CO_2 Perpendicular – Heater On	
	CFD	Series Set Three
20	0.15	0.08
30	0.18	0.14
40	0.21	0.24

TABLE 10
Comparison of CFD Results Against Series Sets Three: Perpendicular Orientation, Heater Off Results

Tunnel Velocity (FPM)	Ventilation Rate (CFM) 0.1 l/min CO_2 Perpendicular – Heater Off	
	CFD	Series Set Three
20	0.15	0.06
30	0.18	0.09
40	0.21	0.17

TABLE 11
Comparison of CFD Results Against Series Sets Six: Parallel Orientation, Heater On (DMH) Results

Tunnel Velocity (FPM)	Ventilation Rate (CFM) 0.1 l/min CO_2 Parallel – Heater On (DMH) Sealed Lip	
	CFD	Series Set Six
20	0.06	0.07
30	0.06	0.07

TABLE 12
Comparison of CFD Results Against Series Sets Six: Parallel Orientation, Heater On (SMO) Results

Tunnel Velocity (FPM)	Ventilation Rate (CFM) 0.1 l/min CO_2 Parallel – Heater On (SMO) Sealed Lid	
	CFD	Series Set Six
20	0.04	0.04
30	0.06	0.04

TABLE 13
Comparison of CFD Results Against Series Sets Six: Perpendicular Orientation, Heater On (SMO) Results

Tunnel Velocity (FPM)	Ventilation Rate (CFM) 0.1 l/min CO_2 Perpendicular – Heater On (SMO) Sealed Lid	
	CFD	Series Set Six
20	0.05	0.05
30	0.06	0.05

TABLE 14
Comparison of CFD Results Against Series Eight Results

Cage Orientation	Ventilation Rate (CFM) 0.1 l/min CO_2 Parallel/ Perpendicular – Heater On (SMO)	
	CFD	Series Set Eight
Parallel	0.10	0.10
Perpendicular	0.09	0.08